

# Nuclear dynamical correlation effects in X-ray spectroscopy from a time-domain perspective

Sven Karsten<sup>1</sup>, Sergei D. Ivanov<sup>1,\*</sup>, Saadullah G. Aziz<sup>2</sup>, Sergey I. Bokarev<sup>1,†</sup> and Oliver Kühn<sup>1</sup>

<sup>1</sup>*Institute of Physics, University of Rostock, Albert-Einstein-Str. 23-24, 18059 Rostock, Germany and*

<sup>2</sup>*Chemistry Department, Faculty of Science, King Abdulaziz University, 21589 Jeddah, Saudi Arabia*

(Dated: July 11, 2021)

To date X-ray spectroscopy has become a routine tool that can reveal highly local and element-specific information on the electronic structure of atoms in complex environments. Here, we focus on nuclear dynamical effects in X-ray spectra and develop a rigorous time-correlation method employing ground state molecular dynamics simulations. The importance of nuclear correlation phenomena is demonstrated by comparison against the results from the conventional sampling approach for gas phase water. In contrast to the first-order absorption, second-order resonant inelastic scattering spectra exhibit pronounced fingerprints of nuclear motions. The developed methodology does not depend on the accompanying electronic structure method in principle as well as on the spectral range and, thus, can be applied to, e.g., UV and X-ray photo-electron and Auger spectroscopies.

PACS numbers: 33.20.Rm, 87.10.Tf, 34.50.Gb, 31.15.A-

*Introduction.* Constant increase of spectral resolution and rapid development of various spectroscopies, covering broad energy ranges from radio frequencies to extra hard radiation, opens new horizons for a molecular scientist to investigate more and more intricate and delicate phenomena. When it comes to obtaining highly local and element-specific information on the electronic structure, X-ray spectroscopies stand out [1]. Popular variants include first order X-ray absorption spectra (XAS) and second order resonant inelastic X-ray scattering (RIXS) techniques. The former focuses on the electronic transitions where a core electron is excited to the manifold of unoccupied molecular orbitals (MOs), whereas the latter detects the emission signal resulting from the re-fill of a core-hole by electrons occupying valence MOs. Although X-ray spectroscopy usually targets electronic transitions, the vibrational ones as well as the accompanying nuclear dynamics have recently received growing attention [2–9]. Remarkably, the RIXS spectra of liquid water and alcohols initiated active ongoing debates in the last decade [10–12], with controversial interpretations, among others involving different aspects of nuclear dynamics [13].

Conventionally, electronic spectra are obtained via single point electronic structure calculations combined with models such as the multi-mode Brownian oscillator one to include broadening on phenomenological level [14]. A big step forward is to sample nuclear distributions in the phase space via molecular dynamics (MD) methods [15–17], leading to a more realistic description of conformational and environmental effects [18–21], although lacking information about correlated nuclear motion. Here, we propose an approach to theoretical calculations of XAS and RIXS spectra based on time-correlation functions obtained from the time evolution provided by electronic ground state MD simulations, analogous to infrared and UV/Vis spectroscopies [14, 17, 22–25].

The central message of this Letter is that nuclear correlation effects are essential for X-ray spectroscopy. We exemplify this on oxygen K-edge spectra of a typical and highly relevant system: gas phase water, by comparison against the results of the aforementioned sampling approach. Importantly, only RIXS, being a second order process, appears sensitive to them, much like non-linear optical spectra provide more detailed insight into the underlying dynamical processes [14, 15].

*Theory.* The proposed method is based on the rigorous derivation from the first principles employing the interaction representation picture and the dynamical classical limit [14, 15]. Technically, the time dependence of all quantities is provided by the classical MD in the electronic ground state. The quantities themselves are obtained from an approximate solution of the time-independent electronic Schrödinger equation at each time instance. The working expressions for XAS,  $\mathcal{X}(\Omega)$ , and RIXS,  $\mathcal{R}(\Omega, \omega)$ , amplitudes can be derived starting from the linear and Raman third-order response functions [14], correspondingly, see Supplement. Note that from the practical standpoint it is more convenient to work in frequency domain.

The XAS process consists of exciting the system from an initial state  $|g\rangle$  to a final core-excited state  $|f\rangle$  by absorbing light with angular frequency  $\Omega$  and polarisation  $\mathbf{e}$ , see left panel in Fig. 1. Similarly, in RIXS the system is first excited to a core-excited intermediate state  $|i\rangle$  or  $|j\rangle$  and then transits to the valence final state  $|f\rangle$  by emitting light with the frequency  $\omega$  and polarisation  $\mathbf{u}$ , see right panel therein. The final expressions for the spectral amplitudes in atomic units read

$$\mathcal{X}(\Omega) = \frac{1}{T} \sum_{g,f} \left\langle \check{M}_f^g(\bar{\omega}_{fg} - \Omega) \check{M}_g^f(\Omega - \bar{\omega}_{fg}) \right\rangle \quad (1)$$

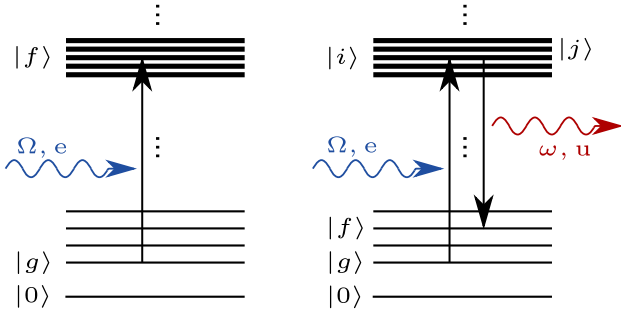


Figure 1: The schematic sketch of XAS (left) and RIXS (right) processes, see text.

and

$$\mathcal{R}(\Omega, \omega) = \frac{1}{T} \sum_{g,f,i,j} \left\langle \int_{-\infty}^{\infty} d\omega_1 \check{M}_j^g(\bar{\omega}_{jg} - [\Omega - \omega_1]) \check{\Delta}_j(\omega_1) \check{M}_f^j([\omega - \omega_1] - \bar{\omega}_{jf}) \int_{-\infty}^{\infty} d\omega_2 \check{M}_i^f(\bar{\omega}_{if} - [\omega - \omega_2]) \check{\Delta}_i(-\omega_2) \check{M}_g^i([\Omega - \omega_2] - \bar{\omega}_{ig}) \right\rangle \quad (2)$$

Here, inversed hats denote the Fourier-transformed quantities and the “dressed” transition dipole moments read

$$\begin{aligned} \bar{M}_g^f(t, 0) &:= D_g^f(t) \exp \left[ i \int_0^t d\tau U_{fg}(\tau) \right] \\ \bar{M}_g^f(t, 0) &:= \mathcal{W}_g(t) D_g^f(t) \exp \left[ i \int_0^t d\tau U_{fg}(\tau) \right], \quad (3) \end{aligned}$$

where  $D_g^f$  are the transition dipole moments from  $|g\rangle$  to  $|f\rangle$  time-evolved with respect to the Hamilton function of the electronic ground state. The gap fluctuation reads  $U_{fg}(\tau) := \Delta E_{fg}(\tau) - \bar{\omega}_{fg}$ , where  $\Delta E_{fg}$  is the electronic energy gap and  $\bar{\omega}_{fg} := 1/T \int_0^T d\tau \Delta E_{fg}(\tau)$  is the mean transition frequency averaged over a trajectory of length  $T$ . Further  $\check{\Delta}_j(\omega') := 1/(2\pi) \sqrt{\Gamma_j/\pi} (\Gamma_j + i\omega')^{-1}$  is the damping function in frequency domain, with  $\Gamma_j$  being the lifetime broadening of the intermediate state  $|j\rangle$ . The lifetimes are thus allowed for by means of a simple phenomenological model accounting for the Auger decay. Additionally, the spectra are convoluted with the Gaussian of width  $\sigma$  along the  $\Omega$ -axis, responsible for the bandwidth of the excitation pulse. Finally, the weighting function

$$\mathcal{W}_g(t) := e^{-\Delta E_{g0}(t)/kT} / \left\langle \sum_g e^{-\Delta E_{g0}(0)/kT} \right\rangle, \quad (4)$$

with  $\langle \dots \rangle$  here and in Eqs. (1,2) standing for the classical canonical average with respect to the Hamilton function of the ground state,  $H_0$ , see Fig. 1. Note that for

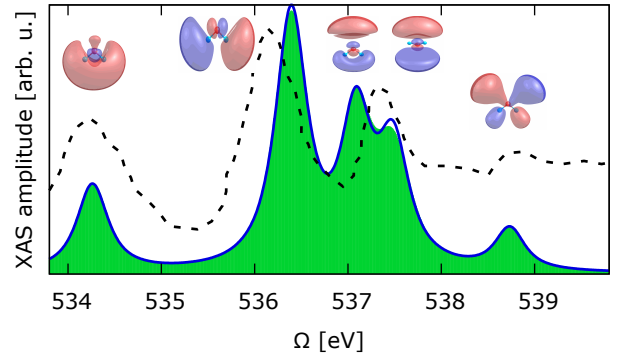


Figure 2: XAS amplitudes for gas phase water. Dashed line represents the respective experimental data from Ref. 26. Blue line depicts the time-correlation approach results according to Eq. (1), whereas filled green curve corresponds to the sampling method. The unoccupied MOs to which the transition is performed are shown near the respective spectral peaks.

the present case of gas phase water, there is only one initial state  $|g\rangle$  that coincides with the ground state  $|0\rangle$ . We note in passing that Eqs. (1,2) can be derived starting from the Fermi’s Golden rule and the Kramers-Heisenberg expression, respectively.

*Computational details.* The MD simulations have been performed using GROMACS ver. 4.6.5 [27] employing the anharmonic qSPC/Fw water model with a Morse O–H potential [28]. A set of 140 uncorrelated initial conditions has been sampled from an *NVT* MD run at 300 K further serving as starting points for *NVE* trajectories. The trajectories have been 0.5 ps long with a timestep of 0.5 fs, yielding a spectral resolution of  $\approx 8$  meV. The electronic Schrödinger equation for each MD snapshot has been solved via ground state density functional theory with the PBE functional [29] using ORCA ver. 3.0.3 [30]. The def2-QZVPP basis set [31] together with (5s5p)/[1s1p] generally contracted Rydberg functions on oxygen have been used. Such a small Rydberg basis does not allow one to reproduce the high-energy tail of the absorption spectrum [32], but enables the description of the lowest states just above the core-excitation threshold. The energies of the valence and core-excited states have been approximated by the differences of the respective Kohn-Sham orbital energies; the corresponding dipole transition moments have been calculated with respect to these orbitals [33], which is known to yield a reasonable compromise between accuracy and efficiency [2, 32–35]. To preserve the continuous time evolution of the dressed dipoles, the entire manifold of relevant electronic levels has been traced along the MD trajectories in a fully-automated manner. The excitation Gaussian linewidth and the uniform Lorentzian lifetime broadening have been chosen as  $\sigma = 0.05$  eV and  $\Gamma = 0.25$  fs $^{-1}$ , respectively. The data have been averaged

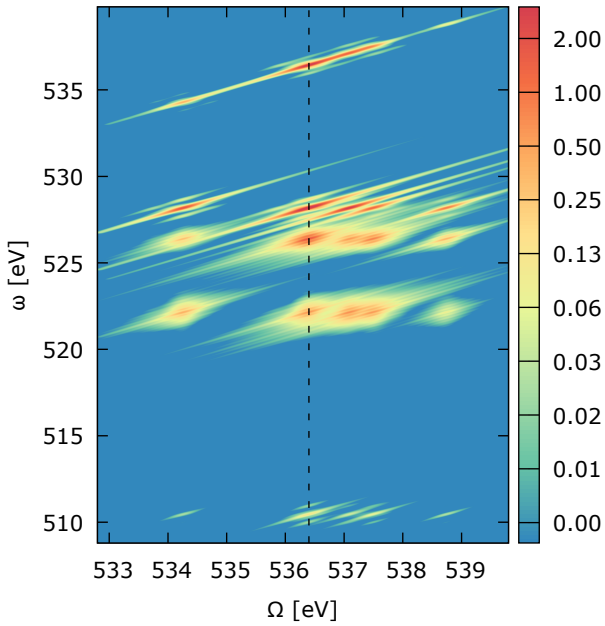


Figure 3: 2D RIXS spectrum,  $\mathcal{R}(\Omega, \omega)$ , of gas phase water obtained by means of the time-correlation approach, Eq. (2); note the log-scale for intensities depicted with color. The dashed vertical line indicates the position of the cut depicted in Fig. 4.

over the molecular orientations assuming the orthogonality of  $\mathbf{e}$  and  $\mathbf{u}$ , which corresponds to a typical experimental setup, and the spectra have been shifted *globally* by 24.8 eV such that the peak structure roughly matches the experimental data [26]. Note that both the sampling and time-correlation approaches employ the same datasets for the consistency of comparison. For further computational details see Supplement.

*Results.* The fingerprints of nuclear correlations are revealed by comparing the spectra obtained via the sampling and correlation approaches. The XAS amplitudes, Fig. 2, are in fairly good agreement with the experimental data [26] shown with the dashed line. We would like to stress that we do not aim at quantitative reproducing and analyzing experimental data with the rather simple but realistic model employed. Instead, the focus is on the nuclear correlation effects, manifesting themselves as the differences between the results of the two aforementioned approaches. The first two absorption peaks correspond to the  $1s_{\text{O}} \rightarrow \sigma^*(2s)$  and  $1s_{\text{O}} \rightarrow \sigma^*(2p)$  transitions, whereas the other three stem from the Rydberg  $1s_{\text{O}} \rightarrow 3p_{\text{O}}$  ones, as is illustrated by the target unoccupied MOs displayed near the respective spectral peaks therein. Apparently, XAS amplitudes feature only subtle differences in intensities between the sampling and the correlation approach. This illustrates the fact that XAS is not a very sensitive observable for nuclear correlation effects.

Figure 3 shows a 2D RIXS spectrum obtained via the

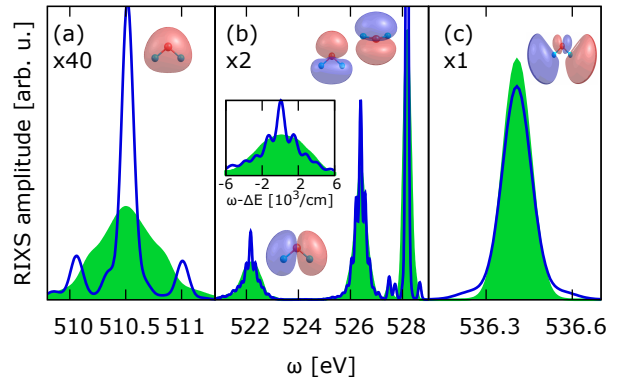


Figure 4: A cut through RIXS spectrum in Fig. 3 at  $\Omega = 536.4$  eV. The color-code is the same as in Fig. 2. Panels depict three relevant spectral ranges. Inset zooms on the left peak in panel (b) that corresponds to  $\sigma(2p) \rightarrow 1s_{\text{O}}$  transition with  $\Delta E = 522.2$  eV.

correlation approach, Eq. (2). Although it gives an overall impression about the spectral shape, it is hard to make quantitative analysis on its basis. Therefore, we consider a particular cut for a fixed excitation frequency  $\Omega = 536.4$  eV that corresponds to the  $1s_{\text{O}} \rightarrow \sigma^*(2p)$  XAS transition, see Fig. 2 and vertical line in Fig. 3. Three spectral ranges shown in Fig. 4 contain peaks related to transitions from the intermediate (core-excited) states to final (ground or valence-excited) ones, see the respective orbitals from which the core-hole refill takes place.

Most importantly, the RIXS spectrum obtained via the time-correlation approach exhibit clear traces of nuclear dynamical effects as compared to the sampling one. First, the two spectra possess notably different lineshapes. For instance, the vibronic structure, which is not present in the sampling spectra by construction, is clearly visible for inelastic features shown in panels (a) and (b) in Fig. 4. In particular the sidebands for peaks at 510.5 eV and 528.2 eV correspond to the O–H stretching mode with the frequency  $3800 \text{ cm}^{-1} \approx 0.47$  eV. Further, the electronic transitions at 522.2 eV (see inset) and 526.4 eV are coupled to the bending vibrational mode having the frequency of  $\approx 1500 \text{ cm}^{-1}$ .

Second, the sampling approach exhibits higher intensity of the elastic peak (panel (c)) and lower intensities of the inelastic ones with respect to the correlation method although both techniques employ the same statistics. The origin of the differences in intensities can be mainly traced back to the complex exponential of the gap fluctuations in the dressed transition dipoles, see Eq. (3), as will be shown in detail elsewhere. We believe that this makes RIXS spectra more sensitive to nuclear dynamical correlation effects, since the expression in Eq. (2) contains energy gap fluctuations between *different* pairs of electronic states. In contrast, the absorption spectrum, Eq. (1), depends only on the initial-final gap fluctuations.

*Conclusions and Outlook.* The simulation protocol allowing for nuclear dynamical phenomena in X-ray spectra has been developed. This rigorously derived method intrinsically exploits molecular dynamics in the electronic ground state together with a phenomenological dephasing model for core-excited states. As a word of caution, using the latter model leaves cases that exhibit intricate large-amplitude dynamics in the excited state, e.g., ultrafast dissociation [36], outside reach. Still, this technique does provide an improvement to the description of nuclear dynamical effects in X-ray spectra. Importantly, these effects have been demonstrated to be essential for X-ray spectroscopy via the comparison against the conventional sampling approach results for gas phase water. Especially RIXS, being a two-photon process, has turned out to be a sensitive technique for the effects in question. In contrast, XAS, being a one-photon process, exhibits no traces of the underlying nuclear dynamics. Interestingly, static (sampling) and dynamic (correlation) nuclear phenomena have been disentangled from each other experimentally, employing RIXS with excitation pulses strongly detuned from the resonance [11]. Thus, a theoretical prediction of fine nuclear effects is expected to stimulate respective high-resolution experiments.

Remarkably, the developed methodology is rather universal and does not conceptually depend on the accompanying electronic structure method. Further, a similar strategy can be applied to the related photon-in/electron-out techniques, such as photo-electron and Auger spectroscopies as well as to other spectral ranges, e.g., UV/Vis. We believe that these developments are especially important in view of the recently suggested non-linear X-ray techniques [37, 38] that are foreseen to be even more informative and sensitive than the conventional RIXS approach.

*Acknowledgement.* We acknowledge financial support by the Deanship of Scientific Research (DSR), King Abdulaziz University, Jeddah, grant No. D-003-435 (S.I.B., O.K.) and the Deutsche Forschungsgemeinschaft KU 952/10-1 (S.K., O.K.), IV 171/2-1 (S.D.I.). Special thanks go to Fabian Gottwald for technical assistance with the MD simulations of water.

---

\* Electronic address: sergei.ivanov@uni-rostock.de

† Electronic address: sergey.bokarev@uni-rostock.de

- [1] J. Stöhr, *NEXAFS spectroscopy*, vol. 25 (Springer Science & Business Media, 2013).
- [2] F. Hennies, S. Polyutov, I. Minkov, A. Pietzsch, M. Nagasono, F. Gel'mukhanov, L. Triguero, M.-N. Piancastelli, W. Wurth, H. Ågren, et al., *Phys. Rev. Lett.* **95**, 163002 (2005).
- [3] M. P. Ljungberg, L. G. M. Pettersson, and A. Nilsson, *J. Chem. Phys.* **134**, 044513 (2011).
- [4] J. E. Rubensson, F. Hennies, and A. Pietzsch, *J. Electron Spectros. Relat. Phenomena* **188**, 79 (2013).
- [5] R. Guillemin, S. Carniato, L. Journal, W. C. Stolte, T. Marchenko, L. E. Khoury, E. Kawerk, M. N. Piancastelli, A. C. Hudson, D. W. Lindle, et al., *J. Electron Spectros. Relat. Phenomena* **188**, 53 (2013).
- [6] W. Dong, H. Wang, M. M. Olmstead, J. C. Fettinger, J. Nix, H. Uchiyama, S. Tsutsui, A. Q. R. Baron, E. Dowty, and S. P. Cramer, *Inorg. Chem.* **52**, 6767 (2013).
- [7] R. Bohinc, M. Žitnik, K. Bučar, M. Kavčič, L. Journal, R. Guillemin, T. Marchenko, M. Simon, and W. Cao, *J. Chem. Phys.* **139**, 134302 (2013).
- [8] A. Pietzsch, Y.-P. Sun, F. Hennies, Z. Rinkevicius, H. O. Karlsson, T. Schmitt, V. N. Strocov, J. Andersson, B. Kennedy, J. Schlappa, et al., *Phys. Rev. Lett.* **106**, 153004 (2011).
- [9] F. Hennies, A. Pietzsch, M. Berglund, A. Föhlisch, T. Schmitt, V. Strocov, H. O. Karlsson, J. Andersson, and J.-E. Rubensson, *Phys. Rev. Lett.* **104**, 193002 (2010).
- [10] K. M. Lange and E. F. Aziz, *Chem. Asian J.* **8**, 318 (2013).
- [11] S. Schreck, A. Pietzsch, K. Kunnus, B. Kennedy, W. Quevedo, P. S. Miedema, P. Wernet, and A. Föhlisch, *Struct. Dyn.* **1** (2014).
- [12] T. Fransson, Y. Harada, N. Kosugi, N. A. Besley, B. Winter, J. J. Rehr, L. G. M. Pettersson, and A. Nilsson, *Chemical Reviews* **116**, 7551 (2016).
- [13] J. A. Sellberg, T. A. McQueen, H. Laksmono, S. Schreck, M. Beye, D. P. Deponte, B. Kennedy, D. Nordlund, R. G. Sierra, D. Schlessinger, et al., *J. Chem. Phys.* (2015).
- [14] S. Mukamel, *Principles of Nonlinear Optical Spectroscopy* (Oxford University Press, Oxford, 1995).
- [15] V. May and O. Kühn, *Charge and Energy Transfer Dynamics in Molecular Systems* (Wiley-VCH, 2011), ISBN 978-3-527-40732-3.
- [16] D. Marx and J. Hutter, *Ab initio molecular dynamics: basic theory and advanced methods* (Cambridge University Press, 2009).
- [17] S. D. Ivanov, A. Witt, and D. Marx, *Phys. Chem. Chem. Phys.* **15**, 10270 (2013).
- [18] Y.-P. Sun, F. Hennies, A. Pietzsch, B. Kennedy, T. Schmitt, V. N. Strocov, J. Andersson, M. Berglund, J.-E. Rubensson, K. Aidas, et al., *Phys. Rev. B* **84**, 132202 (2011).
- [19] N. K. Jena, I. Josefsson, S. K. Eriksson, A. Hagfeldt, H. Siegbahn, O. Björneholm, H. Rensmo, and M. Odellius, *Chem. - A Eur. J.* **21**, 4049 (2015).
- [20] L. Weinhardt, E. Ertan, M. Iannuzzi, M. Weigand, O. Fuchs, M. Bär, M. Blum, J. D. Denlinger, W. Yang, E. Umbach, et al., *Phys. Chem. Chem. Phys.* **17**, 27145 (2015).
- [21] M. Leetmaa, M. Ljungberg, A. Lyubartsev, A. Nilsson, and L. Pettersson, *J. Electron Spectros. Relat. Phenomena* **177**, 135 (2010).
- [22] E. J. Heller, *J. Chem. Phys.* **68**, 3891 (1978).
- [23] S. Lee and E. J. Heller, *J. Chem. Phys.* **71**, 4777 (1979), URL <http://scitation.aip.org/content/aip/journal/jcp/71/12/10.1063/1.438316>.
- [24] C. Lawrence and J. Skinner, *J. Chem. Phys.* **117**, 8847 (2002).
- [25] E. Harder, J. D. Eaves, A. Tokmakoff, and B. Berne, *Proc. Nat. Acad. Sci.* **102**, 11611 (2005).
- [26] K. M. Lange, A. Kothe, and E. F. Aziz, *Phys. Chem.*

- Chem. Phys. **14**, 5331 (2012).
- [27] B. Hess, C. Kutzner, D. van der Spoel, and E. Lindahl, *J. Chem. Theory Comput.* **4**, 435 (2008).
- [28] F. Paesani, W. Zhang, D. A. Case, T. E. Cheatham, and G. A. Voth, *J. Chem. Phys.* **125**, 184507 (2006).
- [29] J. P. Perdew, K. Burke, and M. Ernzerhof, *Phys. Rev. Lett.* **77**, 3865 (1996).
- [30] F. Neese, *Wiley Interdiscip. Rev. Comput. Mol. Sci.* **2**, 73 (2012).
- [31] F. Weigend and R. Ahlrichs, *Phys. Chem. Chem. Phys.* **7**, 3297 (2005).
- [32] L.-Å. Näslund, M. Cavalleri, H. Ogasawara, A. Nilsson, L. G. M. Pettersson, P. Wernet, D. C. Edwards, M. Sandström, and S. Myneni, *The Journal of Physical Chemistry A* **107**, 6869 (2003).
- [33] N. Lee, T. Petrenko, U. Bergmann, F. Neese, and S. DeBeer, *J. Am. Chem. Soc.* **132**, 9715 (2010).
- [34] B. Lassalle-Kaiser, T. T. Boron, V. Krewald, J. Kern, M. a. Beckwith, M. U. Delgado-Jaime, H. Schroeder, R. Alonso-Mori, D. Nordlund, T. C. Weng, et al., *Inorg. Chem.* **52**, 12915 (2013).
- [35] C. J. Pollock, K. Grubel, P. L. Holland, and S. Debeer, *J. Am. Chem. Soc.* **135**, 11803 (2013).
- [36] Y. Harada, T. Tokushima, Y. Horikawa, O. Takahashi, H. Niwa, M. Kobayashi, M. Oshima, Y. Senba, H. Ohashi, K. T. Wikfeldt, et al., *Phys. Rev. Lett.* **111**, 1 (2013).
- [37] J. D. Biggs, Y. Zhang, D. Healion, and S. Mukamel, *J. Chem. Phys.* **136**, 174117 (2012).
- [38] S. Mukamel, D. Healion, Y. Zhang, and J. D. Biggs, *Annu. Rev. Phys. Chem.* **64**, 101 (2013).